VIII International Conference on Fracture Mechanics of Concrete and Concrete Structures
FraMCoS-8
J.G.M. Van Mier, G. Ruiz, C. Andrade, R.C. Yu and X.X. Zhang (Eds)

EXPERIMENTAL STUDY ON THE FRACTURE OF LIGHTLY REINFORCED CONCRETE ELEMENTS SUBJECTED TO ECCENTRIC COMPRESSION

R. PORRAS*, J. R. CARMONA, R. C. YU AND G. RUIZ

Universidad de Castilla-La Mancha (UCLM)
Avda. Camilo José Cela s/n, 13071 Ciudad Real, Spain
*E-mail: Rocio.Porras@uclm.es, www.uclm.es

Key words: Cohesive Fracture, Lightly Reinforced Concrete, Brittle-ductile transition

Abstract. The behavior of lightly reinforced concrete elements under eccentric compression is a complex phenomenon due to material and geometric nonlinearities. This is a field where complete experimental results are lacking. Thus a need was felt to carry out an experimental campaign to investigate the sensitivity of the related parameters on the failure of these type of elements. In this current work, 54 micro-concrete specimens were tested to study the influence of reinforcement amount, slenderness ratio and load eccentricity. The applied load and the displacement at mid-span of the specimen (additional eccentricity) were measured during the entire loading process, including the post-peak stage. At the same time, independent tests were carried out for material characterization. Based on this study, a brittle-ductile classification according to the slenderness ratio and the eccentricity is performed. Such a classification is particularly useful for the element design to avoid brittle failure.

1 Introduction

The buckling failure produced in a reinforced concrete (RC) slender elements, such as columns or panels, is a complex phenomenon. This is due to material and geometrical nonlinearities [1], the bond deterioration between the concrete bulk and the steel rebar [2], the effect of creep [3, 4, 5] as well as the cracking and compressive damage in concrete [6]. All of them lead to stiffness reduction of the column, which in turn exerts a great influence on its buckling failure due to second-order effects [1, 7, 8]. In 1994, Bažant and Kwon studied the size effect in columns [9]. Shortly after that, in 1997, Kim and Yang [10] tested 30 columns made of reinforced high strength concrete (HSC). By changing the slenderness ratio, the concrete strength and the reinforcement ratio, they got the main conclusion that the use of HSC improves the peak load for more stocky columns but has almost no influence on that of the slender ones. In the same year, Foster and Attard [11] observed that the ductility of the column is related to the transverse reinforcement, and that the effectiveness of this reinforcement is heavily influenced by the concrete strength.

All these studies have helped us to understand the phenomenon of buckling in slender RC elements and some variables involved in it. However, given the difficulty of testing elements with a large slenderness ratio, these studies did not take into account all the parameters involved in the fracture process and relevant to the analysis. Thus a need was felt for a complete experimental program in which all material characteristics, including those related to the steel-concrete interaction,

should be measured by direct testing.

In this work, we present the results on the tests carried out on panels of reduced size to facilitate material control and specimen handling, as well as to minimize the data dispersion [12]. All the specimens are weakly reinforced, this entitles us to employ the framework based on fracture mechanics of concrete [13, 14] for result interpretation.

The rest of the paper is structured as follows: a brief overview of the experimental program is given in Section 2. The materials and specimens are described in Section 3. Section 4 summarizes the experimental procedures. The experimental results are presented and discussed in Section 5. Finally, in Section 6 some conclusions are extracted.

2 Overview of the experimental program

The experimental program was designed to study the fracture behavior of lightly RC slender elements. In particular, we want to determine whether this behavior is dependent on the specimen slenderness ratio, the initial load eccentricity and/or the reinforcement amount. In addition, the program had to provide an exhaustive material characterization to allow a complete interpretation of the test results.

As mentioned before, we designed tests on panels of reduced size. This is based on the size effect law described through the Hillerborg's brittleness number

$$\beta_H = \frac{H}{\ell_{ch}}; \ell_{ch} = \frac{EG_F}{f_t^2} \qquad (1)$$

where H is the specimen height, ℓ_{ch} is the characteristic length; E, G_F and f_t are respectively the elastic modulus, the fracture energy and the tensile strength of the concrete. According to the size effect law, two geometrically similar structures will display a similar fracture behavior if their brittleness numbers are comparable [15, 16]. For instance, the behavior of specimens of 30, 60 and 120 mm in height, made from a micro-concrete with a ℓ_{ch} of 90 mm will represent that of specimens of 1, 2 and 4 m made from an ordinary concrete with a ℓ_{ch} of 300 mm.

Therefore tests on fifty-four micro-concrete specimens were carried out. All the specimens were geometrically similar with the same rectangular cross-section of 50×70 mm (B×D), see Fig. 1. Three different heights of 30, 60 and 120 cm were chosen to give slendernesses ratio λ of 21, 42 and 83 respectively, and λ is calculated as follows

$$\lambda = \frac{L_p}{\sqrt{I_y/A}}; I_y = \frac{1}{12}DB^3 \, , A = BD \qquad (2)$$

where L_p is the effective length, which is dependent on boundary conditions, in this case, it is equal to the height H.

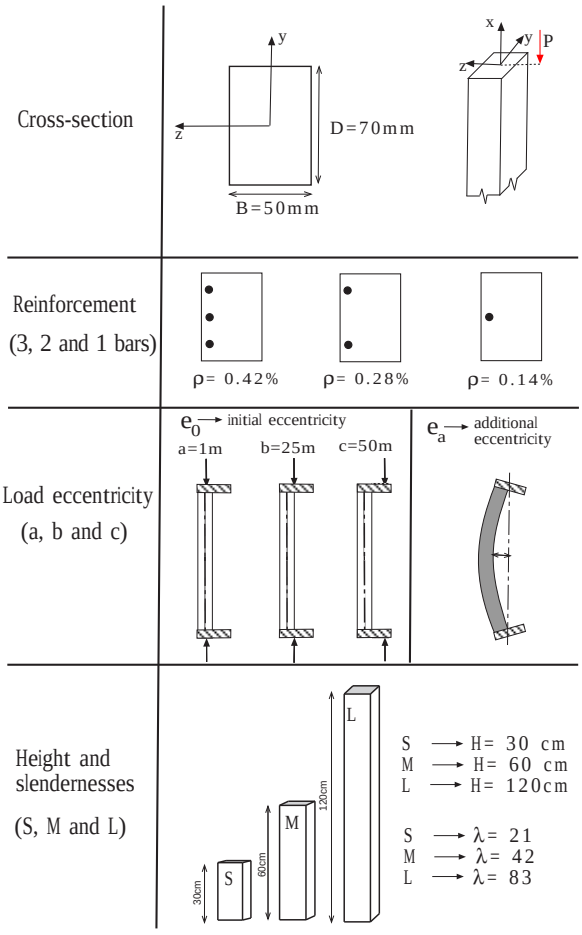

Figure 1: Geometry of the specimens.

The specimens were longitudinally reinforced with one, two or three ribbed steel bars of 2.5 mm in diameter (which resulted

a reinforcement ratio of 0.14%, 0.28% and 0.42% respectively), three settings of the initial load eccentricity, 1, 25 and 50 mm (which we denominated as setting type a, b and c), were applied, see Fig. 1.

Standard characterization and control tests were performed to determine the compressive strength, elastic modulus, tensile strength and fracture energy of the concrete. Steel properties such as the yield strength and the modulus of the steel were obtained from tensile tests. And the steel-to-concrete bond characteristics were determined from pull-out tests in which both the pulling force and the steel slip were measured. The results of all these tests are shown in the next section.

3 Material characterization

3.1 Micro-concrete

A single micro-concrete mix was employed throughout the experiments. The maximum grain size of the siliceous sand was 4 mm and the portland cement was of ASTM type II. All of the cement used was taken from the same cement container and dry stored until use. The mixing proportion by weight were 0.47:3.2:1 (wather:aggregate:cement). The granulometric curve of the aggregate follows UNE 9139.

Nine batches were necessary to cast all the panel specimens plus the necessary characterization specimens. The Abrams cone slump, measured immediately before casting, was of 1.8 cm in average. All the specimens were cast in steel molds, vibrated during 10 seconds while fastened to a vibrating table, wrap-cured for 24 hours, demolded, and right after removal from the moist room, were stored in a moist chamber at 20$\pm$2°C until the test (about 1 month).

Material characterization was carried out on specimens of the same age as the panel specimens. For each batch, four compressive tests were conducted according to ASTM C39 on cylinders of 75 mm in diameter and 150 mm in height. Four Brazilian tests were performed on cylinders of the same dimension, following the procedures recommended by ASTM C496.

The specific fracture energy G_F was measured through three-point bending beams of 75 mm in depth, 50 mm in width and 300 mm in span. The testing procedures followed were according to RILEM TC-50 [17] and with the improvements on the tail part proposed by Elices, Guinea and Planas [18, 19, 20]. Such tests were performed in position control on beam rested on anti-torsion supports. Three linear ramps at different displacements rates were devised: 10 μm/min for the first 25 minutes, 50 μm/min for the following 15 minutes and 250 μm/min until the end of the test.

Table 1: Micro-concrete properties

	f_c [MPa]	E_c [GPa]	f_t [MPa]	G_F [N/m]
Mean	36.5	26.0	3.90	50.7
SD	6.0	4.8	0.53	5.1

The mechanical and fracture properties of the micro-concrete measured are given in Tab. 1. The characteristic length according to Eq. 1 is 93 mm. It needs to be remarked that, the mean values in Tab. 1 are the test results of 36 measurements (four in each batch). The relatively low level of standard deviations among specimens from nine different batches is the outcome of the strict control during the specimen making process.

3.2 Steel

Since the tests were carried out in a reduced scale, in order to achieve the desired reinforcement ratios, the diameter of the steel bars had to be smaller than that of standard rebars. In this case, commercial ribbed wires with a nominal diameter of 2.5 mm were used. The measured characteristics of such wires, such as the nominal elastic modulus E_s, the 0.2% offset yield strength $\sigma_{0.2}$, the ultimate strength σ_u, and the ultimate strain ϵ_u are given in Tab. 2.

Table 2: Reinforcement steel properties

	E_s [GPa]	$\sigma_{0.2}$ [MPa]	σ_u [MPa]	ϵ_u %
Mean	188.0	458.0	603.2	4.3
SD	4.8	24.6	12.4	0.8

3.3 Steel-concrete interface

The stress transfer between steel and concrete was measured through pull-out tests. Thirty-six pull-out tests were performed, four for each batch. Pull-out specimens consist of prisms $75\times75\times150$ mm with a wire embedded along their longitudinal axis. The bonded length was 25 mm to allow a constant shear stress at the interface [21, 22], see Fig. 2 for the experimental setup. The concrete specimen was held by the stiff frame fastened to the machine actuator while the wire was pulled out through a hole in the upper steel plate. The relative slip between the wire and the concrete surface was measured at the bottom end to eliminate the effect of the elastic deformation in the wire. The tests were carried out at a constant displacement of 2 μm/s. The bond strength τ_c, 3.8 MPa in average, is calculated as the measured peak force divided by the contact area.

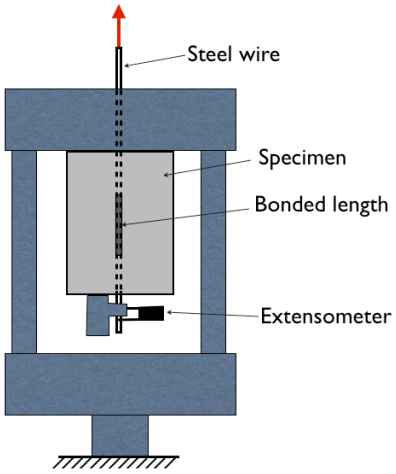

Figure 2: Experimental setup for pull-out tests.

4 Experimental procedure for eccentric compression tests

As mentioned before, fifty-four micro concrete specimens of three sizes (small, medium and large), three reinforcement ratios (one, two and three rebars) and three setting of initial eccentricities (a, b and c for 1, 25 and 50 mm respectively), two for each type, were tested. We name each specimen according to this order, for example, L2b-1 represents a large size specimen with two rebars, loaded with type b setting for the initial eccentricity, and it is the first of the two columns tested.

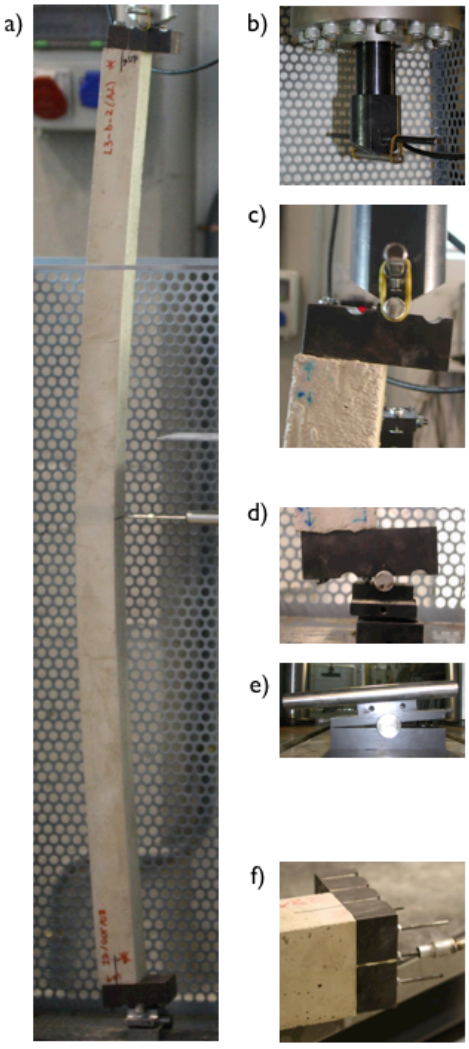

Figure 3: a) Specimen during the test. b-c) Top loading device. d-e) Anti-torsion support. f) Steel block bolted to the specimen for eccentric loading.

All specimens were tested with position control in a vertical position, see the experimental setup in Fig. 3, where the details of the anti-torsion support and the steel block bolted to the specimen for eccentric loading are also depicted. The measure parameters include the applied load P, the loading point displacement d and the additional eccentricity at the midspan of the specimen e_a, see Fig. 4. A servo-controlled testing machine, with a load capacity of 25 kN, was employed for the load application. An inductive transducer, with 20 mm of stroke and 0±2 percent error of its maximum capacity, was used to measure the additional eccentricity.

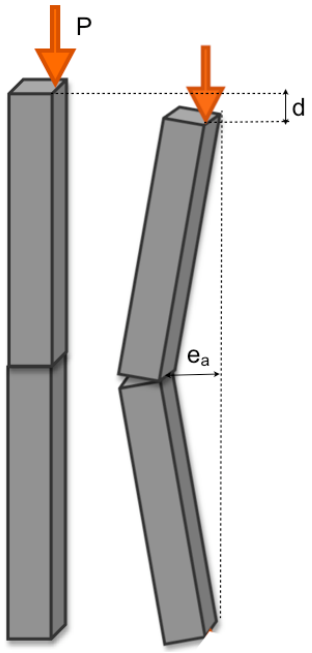

Figure 4: Schematic diagram of the specimens and the measured parameters (applied load P, loading-point displacement d and the additional eccentricity e_a).

5 Experimental results and discussion

The experimental load versus additional eccentricity curves for the RC slender elements are shown in Fig. 5, where the curves are gathered so that the load eccentricity is kept constant for vertical columns and the slenderness ratio for horizontal rows. Each subfigure depicts the curves for 6 specimens of the same size, same type of setting for the load eccentricity and for all three reinforcement ratios, except two results for the smaller specimens were not recorded due to the bolt failure of the loading plate. In addition, the exact values of the initial load eccentricity measured before each test, are also shown below each subfigure.

5.1 Brittle-ductile classification

A typical load-versus-additional-eccentricity curve in Fig. 5 starts with a linear ramp-up. Then a loss of linearity is observed before reaching the peak load, which indicates the initiation of the fracture process. In addition, the peak load decreases with the increase of either the slenderness ratio or the initial load eccentricity. The effect of the two parameters is clarified in Fig. 6, where we put together the curves for small and large specimens, with different settings of initial eccentricity, but all reinforced with one rebar. It can be observed that, for the same size (or slenderness ratio), the increase of initial eccentricity improves the ductility; for the same initial eccentricity, the increase of size also enhances the ductility.

Therefore we have identified two types of behavior in the specimens tested: ductile and brittle. For this purpose, we employ two values of the additional eccentricity, e_{al} and e_a, which correspond to the linearity limit and the peak load respectively, see Fig. 7. The structural behavior is considered as *brittle* if e_a is less than five times e_{al}, *ductile* if e_a is more than ten times e_{al}, *ductile-brittle* if otherwise. The load peak is more pronounced for a brittle type of behavior, whereas the area below the load-eccentricity curve is more extensive for a ductile type of behavior.

It needs to be pointed out that, the reinforcement ratio plays an important role in the above ductile-brittle classification, this is due to the fact that the rebars have yielded at post peak stage. Depending the ultimate load for rebar yielding is larger or not than the peak load, the behavior can stay ductile or change to brittle, see the second row of Fig. 7.

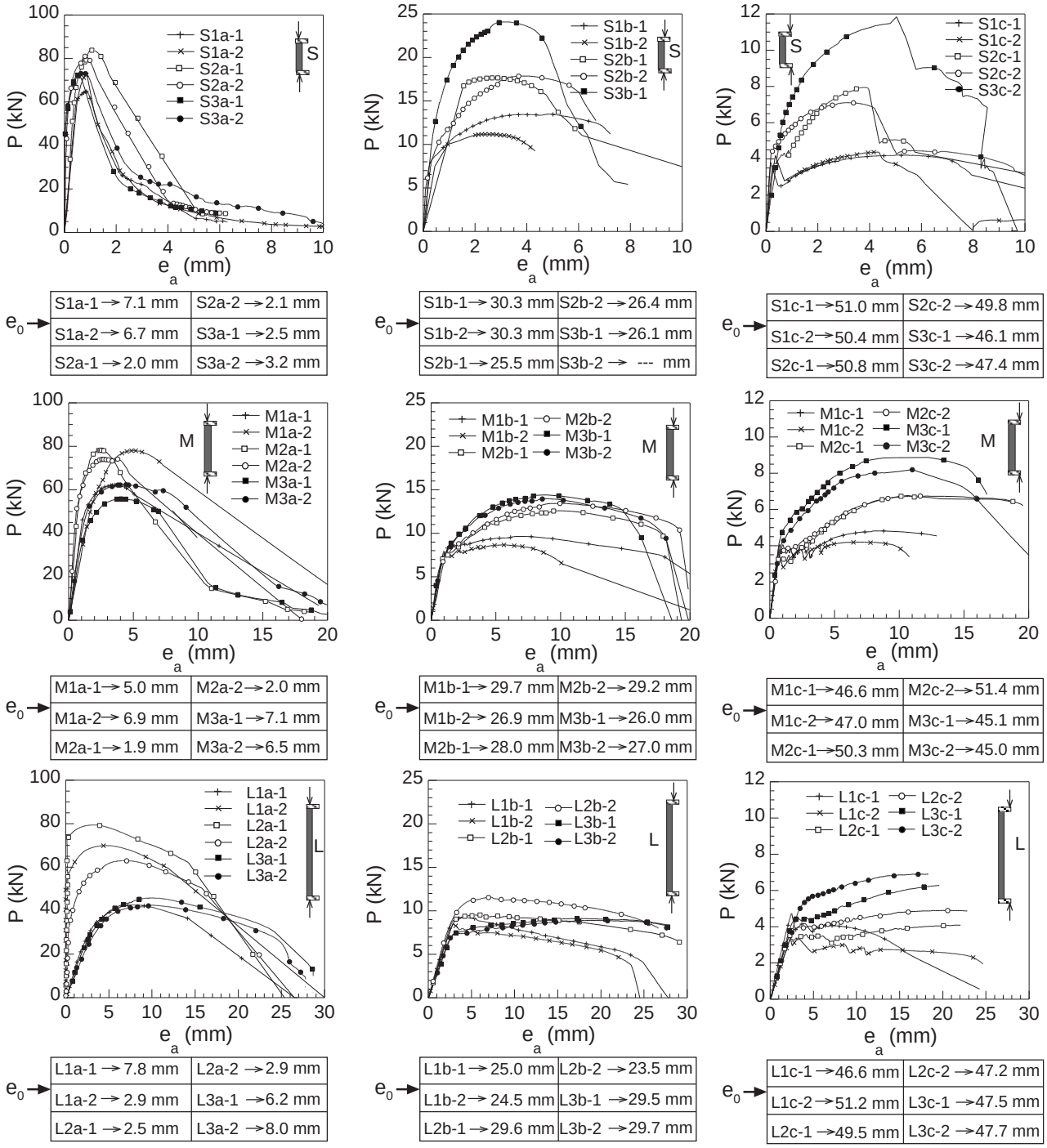

e_0		
S1a-1	7.1 mm	S2a-2 2.1 mm
S1a-2	6.7 mm	S3a-1 2.5 mm
S2a-1	2.0 mm	S3a-2 3.2 mm

e_0		
S1b-1	30.3 mm	S2b-2 26.4 mm
S1b-2	30.3 mm	S3b-1 26.1 mm
S2b-1	25.5 mm	S3b-2 --- mm

e_0		
S1c-1	51.0 mm	S2c-2 49.8 mm
S1c-2	50.4 mm	S3c-1 46.1 mm
S2c-1	50.8 mm	S3c-2 47.4 mm

e_0		
M1a-1	5.0 mm	M2a-2 2.0 mm
M1a-2	6.9 mm	M3a-1 7.1 mm
M2a-1	1.9 mm	M3a-2 6.5 mm

e_0		
M1b-1	29.7 mm	M2b-2 29.2 mm
M1b-2	26.9 mm	M3b-1 26.0 mm
M2b-1	28.0 mm	M3b-2 27.0 mm

e_0		
M1c-1	46.6 mm	M2c-2 51.4 mm
M1c-2	47.0 mm	M3c-1 45.1 mm
M2c-1	50.3 mm	M3c-2 45.0 mm

e_0		
L1a-1	7.8 mm	L2a-2 2.9 mm
L1a-2	2.9 mm	L3a-1 6.2 mm
L2a-1	2.5 mm	L3a-2 8.0 mm

e_0		
L1b-1	25.0 mm	L2b-2 23.5 mm
L1b-2	24.5 mm	L3b-1 29.5 mm
L2b-1	29.6 mm	L3b-2 29.7 mm

e_0		
L1c-1	46.6 mm	L2c-2 47.2 mm
L1c-2	51.2 mm	L3c-1 47.5 mm
L2c-1	49.5 mm	L3c-2 47.7 mm

Figure 5: Load versus additional eccentricity for small (first row), middle (second row) and large (third row) size specimens loaded with eccentricity of 1 mm (left column), 25 mm (central column) and 50 mm (right column). Specific values of the initial eccentricity for each specimen is given below each subfigure.

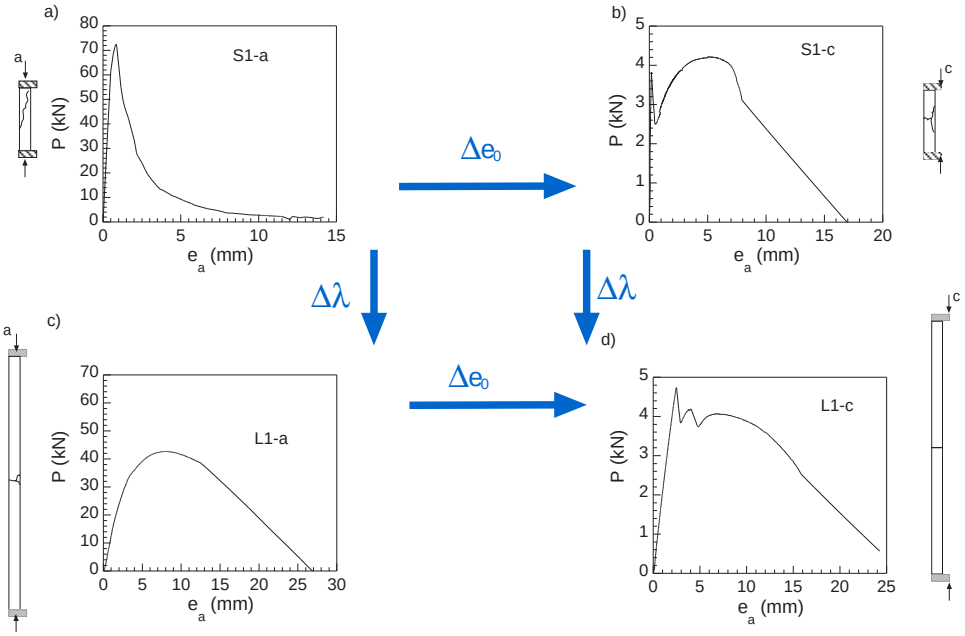

Figure 6: Four typical behavior at post peak, as a function of the initial load eccentricity and the slenderness ratio. The rows are of different size, whereas the columns are of different settings of initial eccentricity.

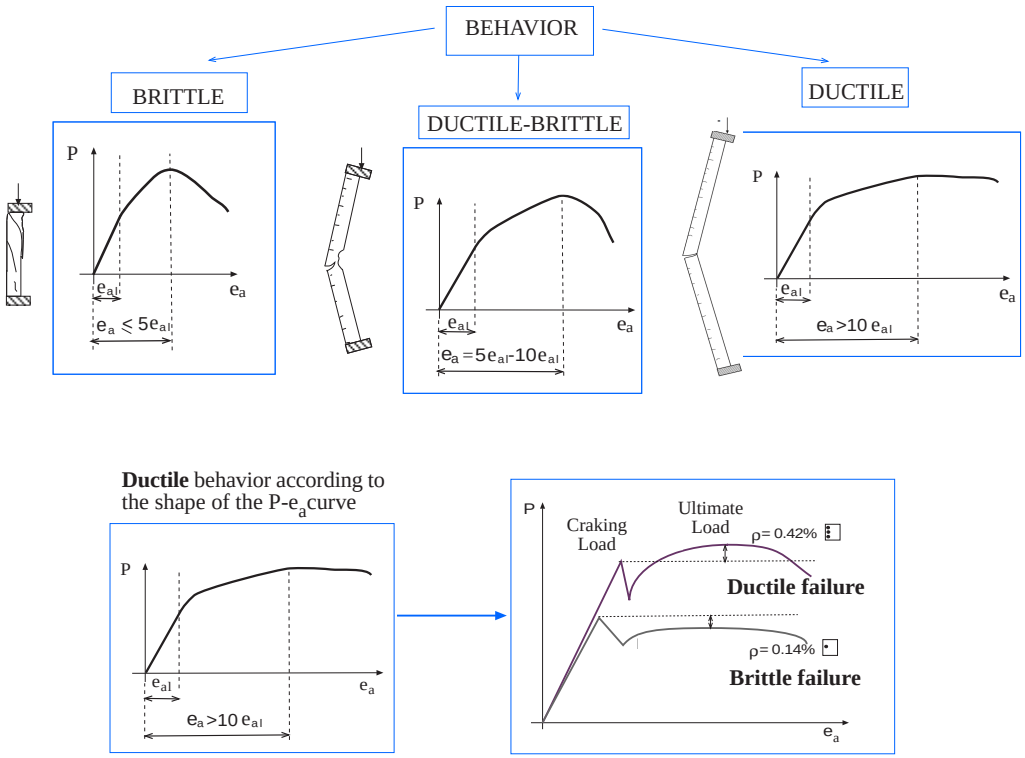

Figure 7: (Top row) Classification criterion for brittle, ductile-brittle and ductile behavior according to relative values of the additional eccentricity at the linearity limit and at the peak load. (Bottom row) Influence of the reinforcement ratio on the failure type (ductile or brittle).

We summarize the previous ductile-brittle classification in Fig. 8, where the initial load eccentricity has been normalized by the specimen thickness, each point represents one specimen tested in the lab. The significance of Fig. 8 lies in the fact that, a given slender reinforced element can be classified as a brittle or ductile structure according to its slenderness ratio and initial load eccentricity.

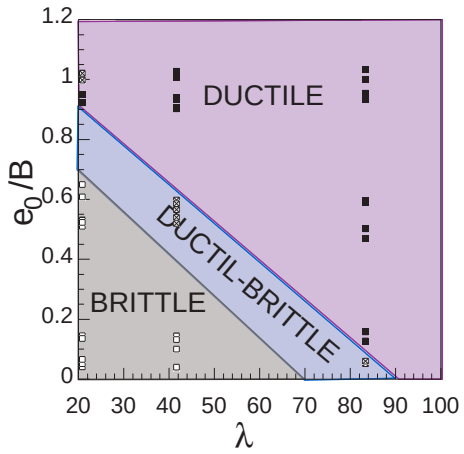

Figure 8: Brittle-ductile transition with respect to the slenderness ratio and the initial load eccentricity normalized by the thickness of the element, note that the ductile region is dependent on the reinforcement ratio.

5.2 Crack patterns

In Fig. 9 we show the typical crack patterns obtained for all the load eccentricity-slenderness ratio combinations in spited of the number of rebars. For the specimens, which structural behaviors have been classified as *brittle*, cracks parallel or inclined to the loading direction are observed; whereas for those specimens, which structural behaviors have been classified as *ductile*, cracks are perpendicular to the longitudinal axis and concentrated around the mid span. In either case, the reinforcement ratio does not play a significant role on the observed crack patterns.

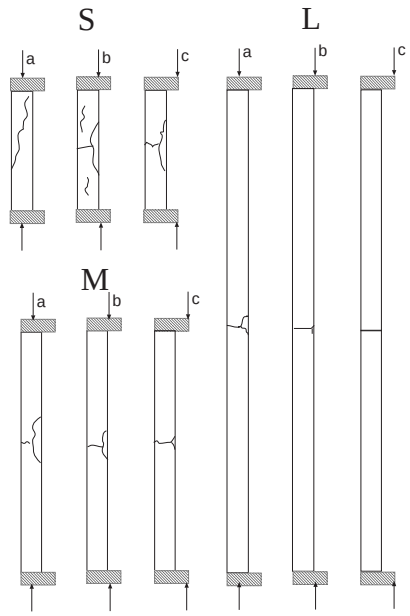

Figure 9: Typical cracking maps for small, medium and large size (S, M and L), and for each three setting of initial load eccentricities (a, b and c.)

6 Summary and conclusions

We have presented experimental results on lightly reinforced concrete slender elements under eccentric compressive load. Geometrically similar specimens and characterizing coupons were cast from a single micro-concrete. Tests were carried out for 54 specimens of three sizes, with three reinforcement ratios and three initial load eccentricity. Material (concrete and steel rebars) and interface properties were measured through independent tests. Concrete-making and testing procedures were strictly controlled to ensure to reduce experimental scatter.

Through analyzing the load-versus-additional-eccentricity curves, we have classified the structural behavior of the tested elements according to their slenderness ratio and initial load eccentricity. It has been observed that the reinforcement ratio plays on an important role on the ductility or brittleness of the structure, but it barely influences the observed crack patterns.

The classification chart obtained provides a guideline to predict the structural behavior for lightly reinforced slender elements.

References

[1] Z. P. Bažant and L. Cedolin. *Stability of Structures*. Dover, Mineola, New York, 2003.

[2] C. Yalcin and M. Saatcioglu. Inelastic analysis of reinforced concrete columns. *Computers and Structures*, 77(5):539–55, 1995.

[3] H. G. Kwak and J. K Kim. Ultimate resisting capacity of slender rc column. *Computers and Structures*, 82:901–915, 2004.

[4] H. G. Kwak and J. K Kim. Nonlinear behaviour of slender RC columns(1). Numerical formulation. *Construction and Building Materials*, 20:527–537, 2006.

[5] H. G. Kwak and J. K Kim. Nonlinear behaviour of slender RC columns(2). Introduction of desing formula. *Construction and Building Materials*, 20:538–553, 2006.

[6] T. Majewski, J. Bobinski, and J. Tejchman. Fe analysis of failure behaviour of reinforced concrete columns under eccentric compression. *Engineering Structures*, 30(2):300–317, 2008.

[7] J.G. McGregor, J.E. Breen, and E.O. Pfrang. Design of slender concrete columns. *ACI Journal*, 67(1):6–28, 1970.

[8] R.W. Furlong. Slenderness of columns in braced frames. *Journal of Structural Div. ASCE*, 119(11):3405–3415, 1993.

[9] Z. P. Bažant and Y. W. Kwon. Failure of slender and stocky reinforced-concrete columns. test of size effect. *Materials and Structures*, 27(166):79–90, 1994.

[10] K.D. Kim and J.K. Yang. Buckling behaviour of slender high-strength concrete colums. *Engineering Structures*, 17:39–51, 1997.

[11] S.J. Foster and M.M. Attard. Experimental test on eccentrically loaded high-strength concrete colums. *ACI Structural Journal*, 94:295–303, 1993.

[12] G. Ruiz, M. Elices, and J. Planas. Experimental study of fracture of lightly reinforced concrete beams. *Materials and Structures*, 31:683–691, 1998.

[13] Z.P. Bažant and J. Planas. Fracture size effect in concrete and other quasibrittle materials. *CRC Press*, 1998.

[14] J.R. del Viso J.R. Carmona, G. Ruiz. Mixed-mode crack propagation through reinforced concrete. *Engineering Fracture Mechanics*, 74:2788–2809, 2007.

[15] L. Elfgren and S.P. Shah, editors. *Analysis of Concrete Structures by Fracture Mechanics: Proceedings of the International RILEM Workshop dedicated to Professor Arne Hillerborg*. RILEM Committee on Fractures Mechanics of Concrete, June 1989.

[16] P. E. Petersson. Crack growth and development of fracture zone in plain concrete and similar materials. *Report No. TVBM-1006, Division of Building Materials, Lund Institute of Technology, Lund, Sweden*, 1981.

[17] RILEM. Determination of the fracture energy of mortar and concrete by means of the three-point bend tests on notched beams. *Materials and Structures*, 18:285–290, 1985.

[18] G.V. Guinea, J. Planas, and M. Elices. Measurement of the fracture energy using three point bend test. 1. influence of experimental procedures. *Materials and Structures*, 25(121-128), 1992.

[19] J. Planas, M. Elices, and G.V. Guinea. Measurement of the fracture energy using three point bend test. 2. influence of

bulk energy dissipation. *Materials and Structures*, 25(305-312), 1992.

[20] M. Elices, G.V. Guinea, and J. Planas. Measurement of the fracture energy using three point bend test. 3. influence of cutting the p-δ tail. *Materials and Structures*, 25(327-334), 1992.

[21] A. Losberg and P. A. Olsson. Bond failure of deformed reinforcing bars based on the longitudinal splitting effect of the bars. *ACI Journal*, 76(1):5–17, 1979.

[22] RILEM/CEB/FIP. Test and specifications of reinforcement for reinforced and prestressed concrete: Four recomendations of the RILEM/CEB/FIB,2: Pullout test. *Materials and Structures*, 3(15):175–178, 1970.